Morphological and Physical Evolutions of Aramid Fibers Aged in a Moderately Alkaline Environment

G. Derombise,[1] L. Vouyovitch van Schoors,[2] A. Bourmaud,[3] P. Davies[4]

[1]*Laboratoire Régional des Ponts et Chaussées de Nancy, CETE de l'Est, Tomblaine, France*
[2]*Materials Department, IFSTTAR, Paris, France*
[3]*Laboratory of Polymers, Properties at Interfaces & Composites, South Brittany-University, Lorient, France*
[4]*Materials & Structures group, IFREMER, Plouzané, France*

Received 3 November 2010; accepted 18 May 2011
DOI 10.1002/app.34923
Published online 2 September 2011 in Wiley Online Library (wileyonlinelibrary.com).

ABSTRACT: The recent use of aramid fibers in geotextiles for ground reinforcement raises fundamental durability issues, in particular in alkaline soils where they are subjected to hydrolysis. To study the degradation mechanisms in such an environment, accelerated aging at pH 9 and at pH 11 has been carried out for up to one and a half years. This work describes the morphological evolutions that occur and the morphology-properties relationship during aging in moderately alkaline environments. The decreases in apparent density are larger at pH 9 than at pH 11, whereas the bulk chemical degradation is more extensive at pH 11 than at pH 9. Scanning electron microscopy micrographs of chemically etched fibers and the measurements of the local elastic modulus by nanoindentation support these results. Finally, this study has indicated an inverse correlation between the porosity level and the tensile strength. © 2011 Wiley Periodicals, Inc. J Appl Polym Sci 123: 3098–3105, 2012

Key words: aramids; fibers; alkaline environment; aging; porosity; SEM; nanoindentation

INTRODUCTION

Twaron 1000 fibers are high performance fibers based on poly(*p*-phenylene terephthalamide) (PPTA, Fig. 1) similar to *Kevlar* fibers.[1] Today, they are proposed in geotextiles for treated soil reinforcement.

Because of the presence of amide-linkages, these fibers are sensitive to hydrolysis.[2,3] The degradation in the presence of water involves a scission of the amide *N*—C linkage, yielding acid and amine functions (Fig. 2).[3,4]

The structure and morphology of PPTA fibers have been studied extensively.[5–10] The highly crystalline and highly oriented structure of PPTA fibers have been shown to be composed of several superimposed structural levels. For example, Panar et al.[5] proposed a structure with a high proportion of extended chains passing through a periodic chain-end layer. Moreover, they highlighted a fibrillar structure, superimposed on the chain-ends structure, consisting of 600-nm wide fibrils oriented in the fiber axis and linked together by tie-fibrils. Finally, these authors showed that the fibrils are uniformly axially oriented in the skin region, whereas the fibrils are imperfectly packed and ordered in the core region. They also suggested that a large proportion of voids are present in the fiber core.

The inherent porosity of *Kevlar 29* and *Kevlar 49* fibers was studied by Dobb et al.[11] by small-angle X-ray scattering (SAXS) and by transmission electron microscopy (TEM). They highlighted that 6-nm wide and 25-nm long rod-shaped microvoids with their long axes approximately parallel to the fiber axis are connected to the surface by a fine capillary network. They suggested that some completely isolated voids are also present in the core. According to these authors, these inherent microvoids would arise during the solidification of the polymer in the coagulating bath of the extrusion process, and would tend to affect the tensile strength of the fibers. Lee et al.[12] determined different void dimensions by SAXS: *Kevlar 29* fibers voids were 10.8-nm wide and 10.6-nm long, whereas *Kevlar 49* fibers voids were 4.7-nm wide and 10.7-nm long. Moreover, they highlighted that the void dimensions of *Kevlar 49* fibers were larger after different hydrolytic treatments. Indeed, they measured voids to be 10.0-nm wide and 10.8-nm long after 40 days under 100% relative humidity (RH) at 125°C, 7.6-nm wide and 11.0-nm long after 14 days under 100% RH at 150°C, and 9.8-nm wide and 8-nm long after 2 days under 100% RH at 200°C. These authors also determined by density measurements that the void fraction increases from 3.38% for as-received *Kevlar 49* fibers to 17.1% after 40 days under 100% RH at 125°C, to 21.4% after 14 days under

Correspondence to: G. Derombise (guillaume.derombise@gmail.com).

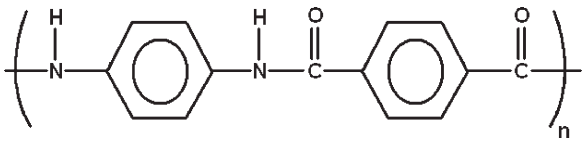

Figure 1 Twaron molecular structure.

100% RH at 150°C, and to 19.0% after 2 days under 100% RH at 200°C. In another study, Dobb and Robson[10] described a defective core where the segments of the pleat structure are interrupted by holes. The authors suggested that the voiding of the core regions results from subsequent loss of solvent from the interior and possibly removal of coagulant during the drying process.[10,11]

Within the framework of a durability study in an alkaline environment, PPTA fibers have been aged at pH 9 and pH 11 for up to one and a half years. The degradation of *Twaron 1000* fibers in moderately alkaline conditions has already been evaluated in previous studies by different techniques (tensile tests, Fourier transformed infrared spectroscopy, viscosimetry, wide-angle X-ray diffraction, size exclusion chromatography etc.).[13,14] In this study, the morphological changes (porosity and surface state) induced by aging will be followed throughout the aging duration, and correlated with the mechanical properties.

EXPERIMENTAL

Materials

The *Twaron type 1000* fiber studied in this article, in the form of 1680 dtex yarn, is a *para*-aramid fiber produced by Teijin Aramid.

Aging methods

Yarns were studied in two aging environments. Yarn samples were immersed in buffer carbonate sodium salt solutions at pH 9 and pH 11. Four temperatures have been considered for each aging condition: 20, 40, 60, and 80°C. Over the aging period considered here the temperature variability is estimated at ±2°C.

Analysis and characterization

Density measurements

The determination of the density of the fibers is based on the Archimedes principle. The samples were successively weighed at 20 ± 1°C in ambient air and once immersed in dodecane, for which the densities are ρ_{air} and $\rho_{dodecane}$, respectively. Then, the density of the fibers, d_{fibers}, was calculated using the following relation:

$$d_{fibers} = \frac{m_1 \times \rho_{dodecane} - m_2 \times \rho_{air}}{m_1 - m_2} \quad (1)$$

where m_1 is the mass weighed in air, m_2 is the mass weighed in dodecane.

The fibers were dried beforehand for 48 h in a vacuum oven at 90°C[15] to remove the water absorbed by the fibers, and then stored at 30°C with silicagel.

Scanning electron microscopy (SEM)

A *Philips XL30* Scanning Electron Microscope was used in the secondary electrons mode, at 12 kV voltage and at a working distance of 10 mm. The surface state of the fibers was observed before and after hydrolytic aging. The fibers were laid on adhesive carbon tabs and then coated with gold. The sections were also examined after one and half minutes immersion in 96% H_2SO_4, at ambient temperature. For this, the fibers were arranged as parallel bundles in epoxy resin, and then cut perpendicularly to their section. The embedded fibers were then polished perpendicularly to their section and coated with gold.

Nanoindentation

For these measurements, the samples were first prepared as for the SEM examinations of the sections described above. Nanoindentation tests involve the contact of an indenter on a material surface and its penetration to a specified load or depth. Load is measured as a function of penetration depth.

In this case, penetration depth is the displacement into the sample starting from its surface. Calculation methods to determine modulus and hardness are based on the work of Oliver et al.[16] The maximum displacement, h_{max}, the maximum load on the sample, P_{max} and the contact stiffness, S, are obtained from the load-penetration curve. S is the slope of the tangent line to the unloading curve at the maximum loading point. The contact depth, h_c is related to the

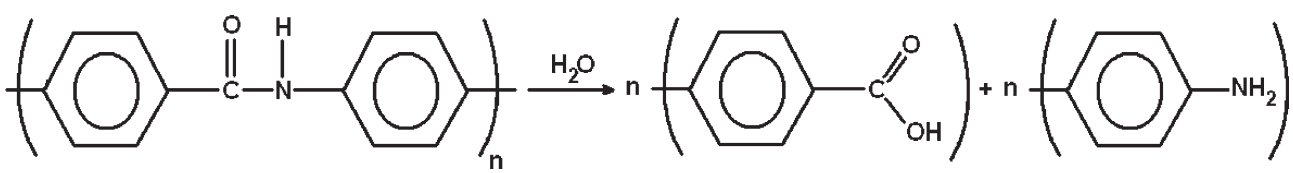

Figure 2 Hydrolysis of PPTA.

deformation behavior of the material and the shape of the indenter:

$$h_c = h_{\max} - \varepsilon \frac{P_{\max}}{S} \quad (2)$$

where ε is a constant that depends on the geometry of the indenter (0.72 for a Berkovich indenter).

For a perfectly sharp Berkovich indenter, projected area a can be calculated by eq. (3) as follows:

$$A = 24.56 h_c^2 \quad (3)$$

The reduced elastic modulus E_r can be calculated with the relationship below:

$$S = 2aE_r = \frac{2\beta}{\sqrt{\pi}} E_r \sqrt{A} \quad (4)$$

where a is the contact radius and β is a constant depending of the geometry of the indenter (1.034 for a Berkovich tip).

The reduced modulus, E_r, which accounts for deformation of both the indenter and the sample is given by:

$$\frac{1}{E_r} = \frac{(1-\nu^2)}{E} + \frac{(1-\nu_i^2)}{E_i} \quad (5)$$

In the above equation, E_i (taken as 1140 GPa) and ν_i (0.07) are the elastic properties of the diamond indenter. E and ν are the elastic modulus and Poisson's ratio of the sample.

Indentation tests were performed with a commercial nanoindentation system (*Nanoindenter XP*, MTS Nano Instruments) at room temperature 23 ± 1°C with a continuous stiffness measurement (CSM) technique. A three-sided pyramid (Berkovich) diamond indenter was employed for the indentation tests.

Strain rate during loading was maintained at 0.05 s^{-1} for all the samples, with 3 nm amplitude, 70 Hz oscillation using identical load rate conditions. The nanoindentation tests were carried out in the following sequence: first, after the indenter made contact with the surface, it was driven into the material with constant strain rate, 0.05 s^{-1} to a depth of 120 nm; secondly, the load was held at maximum value for 60 s; and finally, the indenter was withdrawn from the surface with the same rate as during loading.

The indentation measurements were performed approximately every micrometer along a diameter of the fiber sections (Fig. 3), which represents around 13 measurements per section.

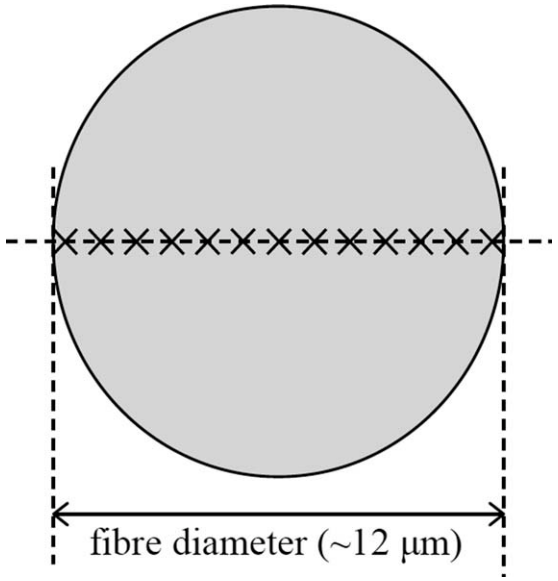

Figure 3 Fiber transversal section. The crosses along the diameter line represent the indentation measurements.

RESULTS AND DISCUSSION

Density changes

The presence of finish has been shown to have a significant influence on the density of the *Twaron* fibers.[17] Indeed, the relative density is 1.445 ± 0.005 for fibers with 0.14 wt % finish content (*Twaron 1010*), whereas it is 1.425 ± 0.019 for fibers with 0.6–1 wt % finish content (*Twaron 1000*). These values are similar to those reported by Teijin Aramid.[18] To take into account this finish effect, a correction was performed using FTIR-ATR data. After identifying the peak related to the finish, evaluating the remaining finish content at different aging time, an "apparent" density, d^*, related to the density of the polymer only (without any finish content), has been determined.

$$d* = \frac{M_{\text{polymer}} d_{\text{fiber}}}{\frac{M_{\text{polymer}} d_{\text{fiber}}}{d_{\text{polymer}}} + 1 - d_{\text{fibre}} \left(\frac{M_{\text{finish}}}{d_{\text{finish}}} + \frac{M_{\text{polymer}}}{d_{\text{polymer}}} \right)} \quad (6)$$

where M_{polymer} and M_{finish} are the weight percentages of the polymer and the finish, respectively, d_{fiber} is the measured density and d_{polymer} is the density of the polymer alone (without any finish). d_{polymer} has been assumed to be equal to the density of the as-received *Twaron 1010* fibers after removing the residual finish content. The calculation is detailed elsewhere.[14]

The apparent density evolution at pH 9 and pH 11 after one year aging are reported in Figure 4 and Table I.

Figure 4 indicates that the apparent density of *Twaron 1000* fibers aged at pH 11 remains constant at 20°C, and decreases slightly at 80°C. At pH 9, the apparent density follows a logarithmic evolution with time. A short-term closed porosity development thus occurs under the latter conditions. The standard deviation of the density of as-received fibers is much

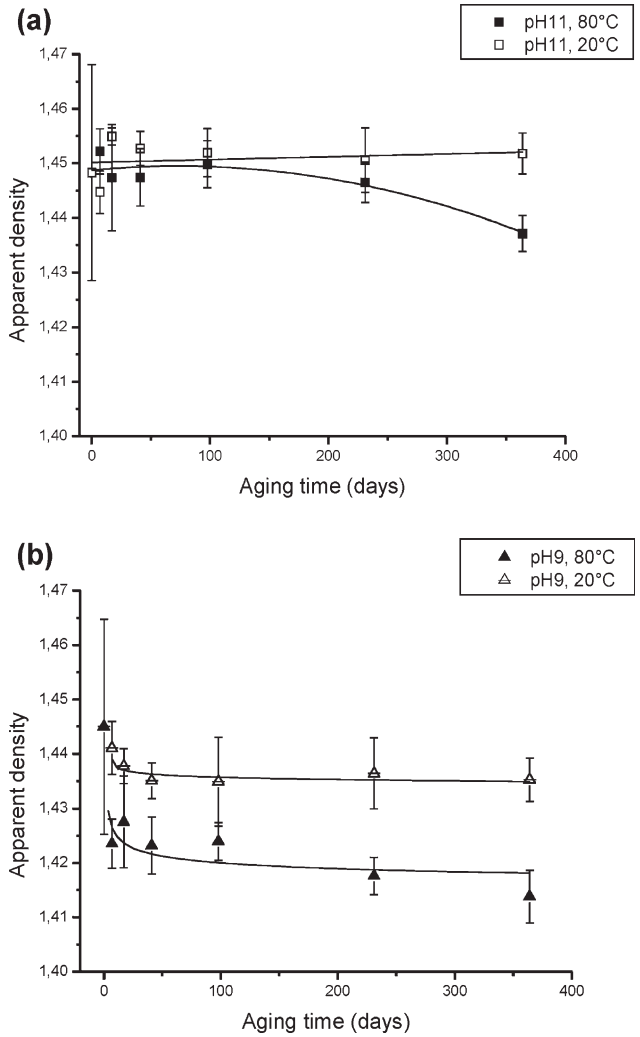

Figure 4 Evolution of the apparent density of *Twaron 1000* fibers aged (a) at pH 11 and (b) at pH 9.

larger than for aged materials, probably due to some variation of the finish content application along the yarns. From Table I, it appears that the apparent density of *Twaron 1000* fibers aged at pH 9 is lower than for those aged at pH 11, for the same aging temperature. It must be mentioned that the porosity development trends observed here differ from the chemical degradation evolutions followed in another study.[13] Indeed, it has been previously shown that the reduced viscosity at 2.10^{-3} g/mL, which is directly related to the weight average molecular mass, decreases by $\sim$ 20% at pH 9 and 80°C and by $\sim$ 80% at pH 11 and 80°C, after 1 year aging.[13] However, the porosity development and the chemical degradation are both accelerated by the temperature. In fact, the reduced viscosity at 2.10^{-3} g/mL decreases by <3% after 1 year aging at 20°C, both at pH 11 and at pH 9. These results reveal that the porosity development at pH 9 and at pH 11 depends on different processes.

Morgan and Pruneda[19] and Penn and Larsen[20] detected some residual Na_2SO_4 impurities in the *Kevlar 49* fibers introduced during the manufacturing process. The former suggested that these are in the form of small clusters that get trapped in the interfibrillar regions upon shrinkage during the fiber drying stage.[19] They speculated that the Na_2SO_4 impurities are a source of microvoid formation, particularly in the latter stages of drying when trapped aqueous Na_2SO_4 concentrations impose osmotic pressure on the surroundings.

The higher chemical degradation level observed at pH 11[13] may favor a development of pathways into the structure that would permit the aging solution to diffuse more easily. Under these conditions, the residual impurities, which may be a source of microvoid formation,[19] would be washed out at pH 11 to a greater extent than at pH 9. This mechanism may contribute to a higher porosity development at pH 9 than at pH 11. However, further work is needed to confirm this.

It is important to examine how the development of porosity observed at pH 9 affects the mechanicals properties in tension. First, the normalized tensile strength and the apparent density of *Twaron 1000* fibers aged at pH 9 have been plotted in Figure 5. The evolution of the tensile strength with aging time for the different conditions has been reported in a previous study.[13]

It appears that the apparent density and the tensile strength are correlated: the lower the apparent density, the higher the porosity level, and the lower the tensile strength, as suggested by Dobb et al.[11] A second order polynomial relation can fit the data to a first approximation.

In another study,[13] we have shown that the tensile strength and the reduced viscosity measured at 2×10^{-3} g/mL (which is correlated with the chain length) of *Twaron 1000* fibers aged at pH 11 are linearly correlated. It has been noted that the fibers aged at pH 9 deviate slightly from this linear relation: for the same chain degradation rate (that is to say for the same reduced viscosity at 2×10^{-3} g/mL), the tensile strength loss is larger at pH 9 than at pH 11. The development of bulk porosity at pH 9 may explain this trend. This result would confirm that

TABLE I
Apparent Density Values of *Twaron 1000* Fibers After 1 Year Aging at pH 11 and at pH 9

		Apparent density
As-received		1.449 ± 0.020
pH11	20°C	1.449 ± 0.004
	80°C	1.434 ± 0.003
pH9	20°C	1.435 ± 0.004
	80°C	1.414 ± 0.005

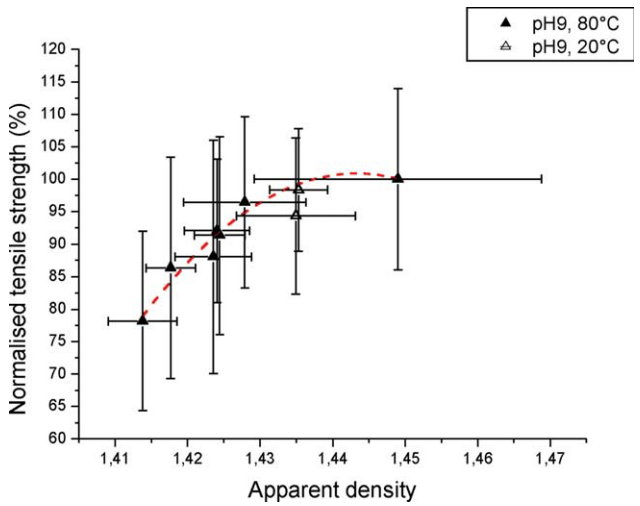

Figure 5 Normalized tensile strength versus the apparent density of *Twaron 1000* fibers aged at pH 9 for up to 1 year. [Color figure can be viewed in the online issue, which is available at wileyonlinelibrary.com.]

the porosity affects the tensile strength, as suggested by Morgan et al.[6]

To examine the presence of void regions, SEM observations both of the surface state and of the fiber sections after a H_2SO_4 treatment were carried out.

Morphological examinations

Surface state

Figure 6 groups the SEM micrographs of *Twaron* fibers before and after 1 year aging in an alkaline environment.

The surface of *Twaron 1000* as-received fibers is smooth and does not display any defects [Fig. 6(a)]. After 1 year at pH 9 and 80°C, the fibers display some local finish rearrangement and some fibril removal leaving longitudinal grooves at the surface [Fig. 6(b)], attributed to abrasion probably due to the stirring of the aging solutions. After 1 year at pH 11 and 80°C, the fibers present some local randomly oriented hexagonal shapes [Fig. 6(c)], which may be due to rearrangement of some drawing agent embedded in the surface. It must be emphasized that the diameter remains constant for all conditions. No evidence of open porosity can be seen on these surface state SEM micrographs.

H_2SO_4-etched sections

Hydrochloric acid-etching is a well-known technique used to study the structure of polymer fibers by revealing defects or amorphous regions.[5–7] Indeed, HCl-etching via chain hydrolysis will preferentially occur in less perfect crystalline regions as a result of greater diffusion and solubility of the acid in such regions.[6] We have thus immersed *Twaron 1000* as-received fibers for five weeks in HCl 37% at ambient temperature. As the surface and the cross section remain intact after this treatment, the fibers were immersed for one and a half minutes in 96% H_2SO_4,

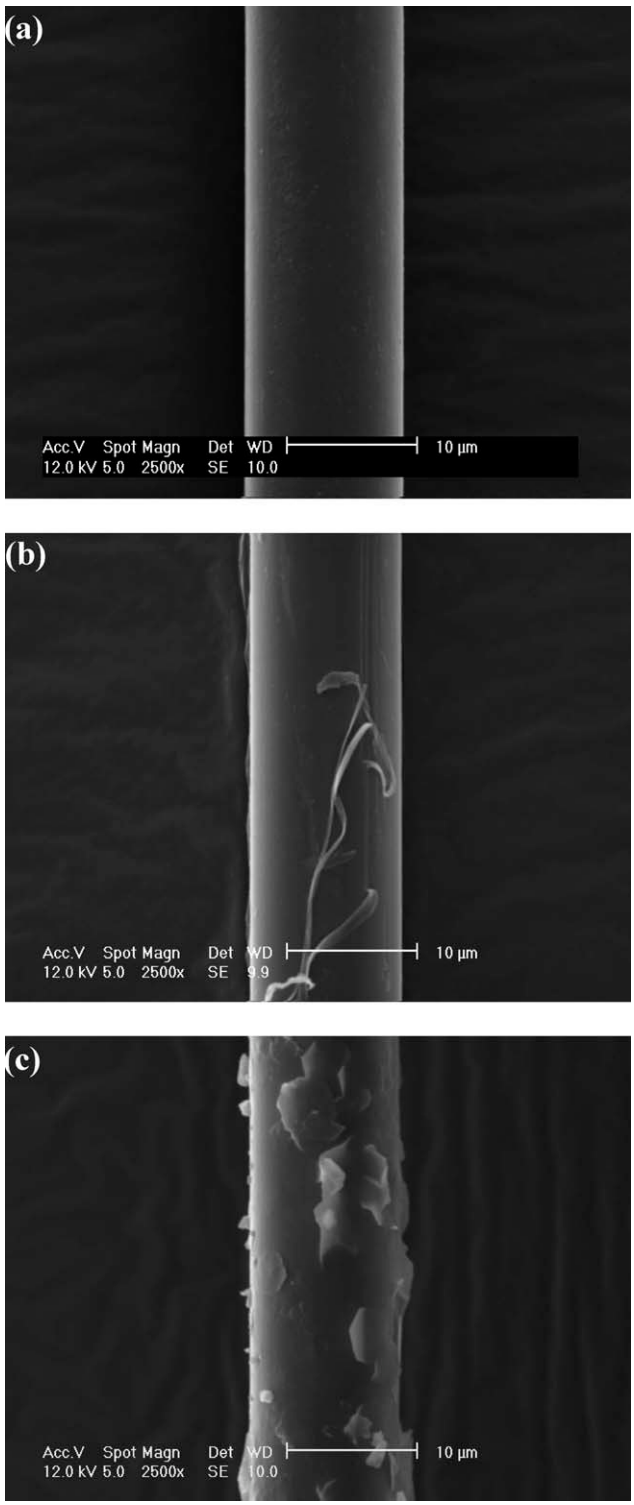

Figure 6 SEM observations of *Twaron 1000* fibers (a) as-received, (b) after 1 year at pH 9 and 80°C, and (c) after 1 year and at pH 11 and 80°C.

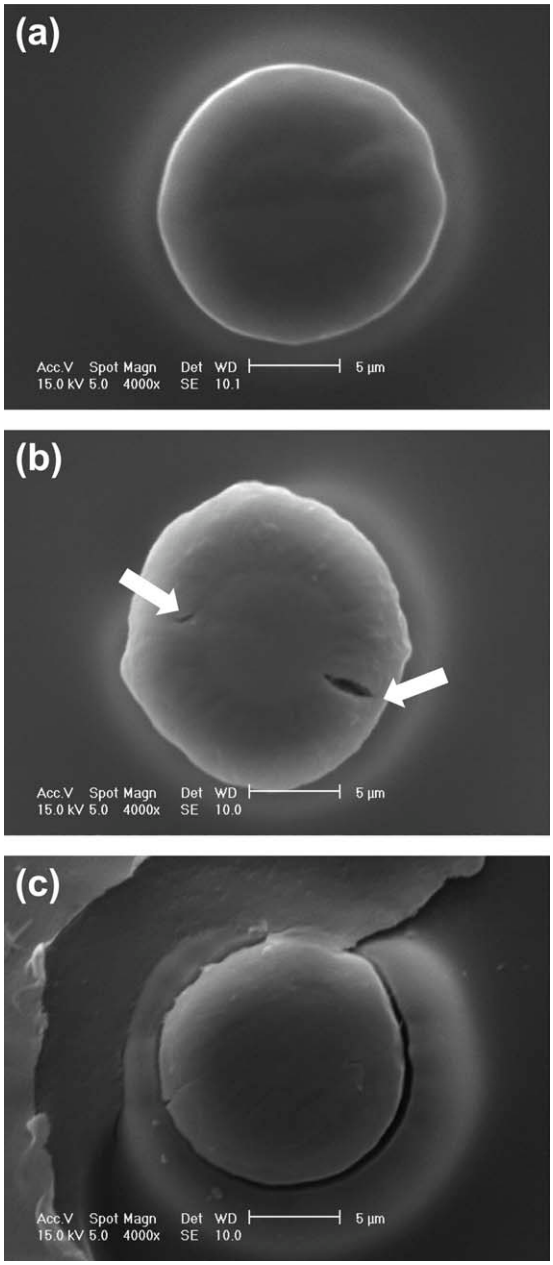

Figure 7 Sections of *Twaron 1000* fibers (a) as-received, (b) after 1 year at pH 9 and 80°C, and (c) after 1 year at pH 11 and 80°C, observed by SEM after one and half minutes immersion in H_2SO_4 (96%) at ambient temperature. The white arrow indicates the presence of porosity-rich regions.

which is a solvent for PPTA fibers. It is likely that the less perfect crystalline and more exposed regions will be dissolved first.

Figure 7 groups some representative SEM micrographs of H_2SO_4-etched sections of *Twaron 1000* fibers before and after 1 year aging in an alkaline environment. Several fibers were studied for each condition. All the pictures presented here have been taken after the same H_2SO_4 treatment. It should therefore be noted that the morphology of H_2SO_4-etched sections strongly depends on the time of immersion and they are not very reproducible.

The sections of as-received fibers are smooth and do not seem to be affected by the H_2SO_4 treatments [Fig. 7(a)]. In a similar way, the sections of fibers aged during 1 year at pH 11 and 80°C do not display any defects [Fig. 7(c)]. However, the sections of fibers aged for 1 year at pH 9 and 80°C [Fig. 7(b)] display some holes with an ellipsoidal cross section, for which the larger diameter is oriented in the radial directions. These holes are located in the core of the fibers, and are most probably in the interfibrillar regions, as suggested by Morgan and Pruneda.[19]

These observations support the different evolutions of the apparent density depending on the aging conditions: there would be some development of porosity under aging at pH 9, whereas it would be insignificant at pH 11.

Nanoindentation experiments have been performed to confirm these results.

Nanoindentation

Nanoindentation experiments were performed on *Twaron 1000* fibers before and after one and a half years aging at pH 9 and 80°C or at pH 11 and 80°C. Figure 8 groups the modulus measurements by nanoindentation along a fiber diameter.

First, for all conditions, it appears that the measured modulus is slightly higher at the edges of the fiber diameter, except for the fibers aged at pH 11 and 80°C. Two interpretations can be proposed:

- It may be due to a denser structure and a better orientation in the fiber skin than in the core, as proposed by several authors.[5,6,10] Even if the skin thickness can not be determined precisely from these measurements, it may be concluded that the "skin effect" is not wider than 1 µm,

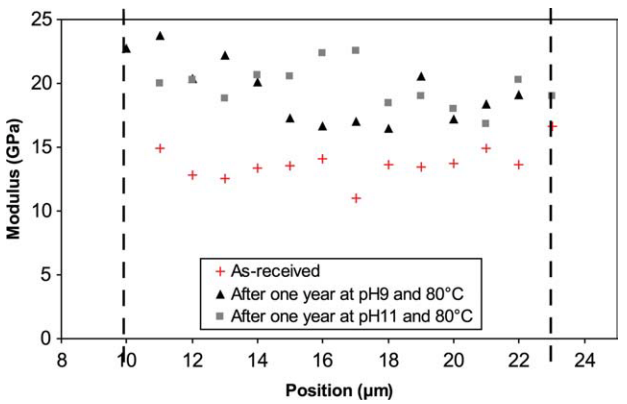

Figure 8 Evolution of the modulus measured by nanoindentation along the fiber diameter. The dashed lines represent the fiber extremities. [Color figure can be viewed in the online issue, which is available at wileyonlinelibrary.com.]

which would be in accordance with Dobb and Robson's observations.[10] These authors measured the skin thicknesses of different PPTA fiber grades, from TEM observations of silver sulfide impregnated fibers. They determined a skin thickness varying from 0.3 to 1 μm for *Kevlar 29* and *Kevlar 49* fibers (for a diameter of 12.6 μm and 12.1 μm, respectively), and a skin of 0.15 μm for *Twaron* fibers (for a diameter of 12.5 μm).

- The higher modulus at the fiber extremities may also be attributed to the filling of microvoids located in the outer regions by the liquid epoxy resin, as showed by Lee et al.,[12] during the sample preparation.

It appears that the elastic modulus is higher for hydrolytically aged fibers than for as-received fibers. In a previous study, we showed by wide-angle X-ray scattering (WAXS) that the lateral apparent crystallite size (ACS) increases significantly (from 6 to 7% for ACS_{110}) for *Twaron 1000* fibers aged for 1 year at pH 11 and at pH 9, at 80°C.[14] This increase in the lateral ACS was attributed to the recrystallization of lateral "links," such as tie-fibrils, tie-molecules or imperfectly crystallized chains, at the surface of pre-existing crystallites. As imperfectly crystallized material further crystallizes during aging, the increase in the lateral ACS may be thus regarded as an increase in "lateral crystallinity." The higher modulus measured by nanoindentation after aging may be caused by the increase in the "lateral crystallinity" for hydrolytically aged *Twaron 1000* fibers, as suggested by Beake and Leggett for poly(ethylene terephthalate films).[21] It should be noted that the local properties measured by nanoindentation are not representative of the global tensile properties, as the axial tensile modulus (measured between 0.3 and 0.6% strain) of *Twaron 1000* fibers has been shown to remain constant throughout the aging duration, for all the conditions considered here.[13] Moreover, it can be noted that the elastic modulus values measured by nanoindentation are not in the same range as the elastic modulus determined by tensile tests ($\sim$ 80 GPa for the tensile modulus). This may be due to a "scale effect": as the indenter penetrates into the structure, it may separate the fibrils by breaking some lateral links (such as the "tie-fibrils" described by Panar et al.[5]) resulting in lower elastic modulus.

Finally, Figure 8 illustrates that the local elastic modulus of aged fibers depends on the pH, and on the location along the diameter line. Indeed, for the fibers aged in the two conditions, the modulus values are in a similar range up to $\sim$ 4 μm from the border of the fibers. In the center, beyond $\sim$ 4 μm from the border, the modulus is significantly lower for the fibers aged at pH 9 and 80°C. In various fields of materials science, it has been established that the higher the porosity level, the lower the elastic modulus measured by nanoindentation.[22–28] The trend observed here may thus be related to the higher closed porosity development at pH 9 and 80°C than at pH 11 and 80°C.

Based on these results and interpretations, the modulus measured by nanoindentation may result from a combination of an increase in the crystallinity, which would increase the modulus value, and an increase in the porosity level, which would reduce it.

CONCLUSIONS

Twaron 1000 fibers have been aged in a moderately alkaline environment for up to one and a half years. The evolution of the apparent density has been evaluated throughout the aging duration and has been shown to depend on the aging condition.

At pH 11, the apparent density decreases slightly after 1 year aging at 80°C, whereas it remains constant at 20°C. This result is supported by a porosity development observed on H_2SO_4-etched sections.

At pH 9, the apparent density decreases significantly after 1 year aging at 80°C. In the same way, this result is supported by a porosity development observed on H_2SO_4-etched sections. The apparent density decreases slightly after one year aging at pH 9 and 20°C.

Nanoindentation measurements show that the local elastic modulus of the inner regions is lower after aging at pH 9 and 80°C than after aging at pH 11 and 80°C. Moreover, the elastic modulus of as-received fibers is significantly lower than for the hydrolytically aged fibers. The trends observed here have been explained by a combination of an increase in the crystallinity and an increase in the porosity level.

Finally, this study has indicated an inverse correlation between the porosity level and the tensile strength. Further analyses, such as SAXS, would enable this effect to be quantified.

The authors are grateful to Otto Grabandt and Bertil van Berkel (Teijin Aramid) for the fiber samples and their cooperation. The high commitment of Dominique Duragrin (IFSTTAR) for the density measurements is also greatly appreciated.

References

1. Yang, H. H. Kevlar Aramid Fiber; John Wiley & Sons: New York, 1993.
2. Auerbach, I. J Appl Polym Sci 1989, 37, 2213.
3. Morgan, R. J.; Pruneda, C. O.; Butler, N.; Kong, F.-M.; Caley, L.; Moore, R. L.Proceedings of the 29th National SAMPE Symposium 1984, 891.
4. Mercier, J. P.; Maréchal, E.; Chimie Des Polymères: Synthèses, Réactions, Dégradations; Presses Polytechniques et Universitaires Romandes, 1993; Chapter 10.

5. Panar, M.; Avakian, P.; Blume, R. C.; Gardner, K. H.; Gierke, T. D.; Yang, H. H. J Polym Sci Polym Phys 1955, 1983, 21.
6. Morgan, R. J.; Pruneda, C. O.; Steele, W. J. J Polym Sci Polym Phys 1983, 21, 1757.
7. Li, L.-S.; Allard, L. F.; Bigelow, W. C. J Macromol Sci Phys 1983, B22, 269.
8. Dobb, M. G.; Johnson, D. J.; Saville, B. P. J Polym Sci Polym Symp 1977, 58, 237.
9. Dobb, M. G.; Johnson, D. J.; Saville, B. P. J Polym Sci Polym Phys 1977, 15, 2201.
10. Dobb, M. G.; Robson, R. M. J Mater Sci 1990, 25, 459.
11. Dobb, M. G.; Johnson, D. J.; Majeed, A.; Saville, B. P. Polymer 1979, 20, 1284.
12. Lee, J. S.; Fellers, J. F.; Tang, Y. J Compos Mater 1985, 19, 114.
13. Derombise, G.; Vouyovitch Van Schoors, L.; Davies, P. J Appl Polym Sci 2010, 116, 2504.
14. Derombise, G.PhD Thesis, École des Ponts ParisTech, 2009.
15. Saijo, K.; Arimoto, O.; Hashimoto, T.; Fukuda, M.; Kawai, H. Polymer 1994, 35, 496.
16. Oliver, W. C.; Pharr, G. M. J Mater Res 1992, 7, 1564.
17. Derombise, G.; Vouyovitch Van Schoors, L.; Messou, M.-F.; Davies, P. J Appl Polym Sci 2010, 117, 888.
18. Teijin. Twaron, the Power of Aramid—Twaron for Heat and Cut Protection. Sales brochure.
19. Morgan, R. J.; Pruneda, C. O. Polymer 1987, 28, 340.
20. Penn, L.; Larsen, F. J Appl Polym Sci 1979, 23, 59.
21. Beake, B.; Leggett, G. Polymer 2002, 43, 319.
22. Deng, X.; Koopman, M.; Chawla, N.; Chawla, K. K. Mater Sci Eng 2004, A364, 240.
23. Fougere, G. E.; Riester, L.; Ferber, M.; Weertman, J. R.; Siegel, R. W. Mater Sci Eng 1995, A204, 1.
24. Gross, K.; Saber-Samandari, S. Surf Coat Technol 2009, 203, 2995.
25. Jang, B.-K.; Matsubara, H. Mater Lett 2005, 59, 3462.
26. Krell, A.; Schädlich, S. Mater Sci Eng 2001, A307, 172.
27. Ling, Z.; Wang, X.; Ma, J. Mater Sci Eng 2008, A483, 285.
28. Velez, K.; Maximiliene, S.; Damidot, D.; Fantozzi, G. Cement Concrete Res 2001, 31, 555.